

# A Novel Spherical Joint Designed for Metamorphic Mechanism

Weihai Chen<sup>a</sup> Jianbin Zhang<sup>β</sup> Junjie Quan<sup>β</sup> Tao Lv<sup>β</sup>

<sup>a</sup>School of Automation Science and Electrical Engineering  
Beijing University of Aeronautics and Astronautics  
Beijing 100083, China.  
whchenbuaa@126.com jbzhangbuaa@163.com

<sup>β</sup>School of Mechanical Engineering  
Beijing University of Aeronautics and Astronautics  
Beijing 100083, China.  
qjjccairforce@tom.com longjue1984@sina.com

**Abstract**— A novel design of passive spherical metamorphic joint is proposed in this paper, the special mechanism of this design allows multi links to be connected together to do spherical motion about a rotation center. The main contribution of the joint design is the offset parallelogram mechanism and a couple door joints, which can overcome efficiently the inherent defect from the conventional spherical joint design where a spherical joint can only connect two links simultaneously to do the motion. With this novel joint, we construct a kind of special six-bar spherical metamorphic mechanism. It is also explained how to do the configuration analysis, and to find the adjacency matrix of the metamorphic mechanism. According to the characteristic of the joint, some typical applications have been illustrated through parallel and variable geometry truss manipulators.

**Keywords**— spherical metamorphic mechanism, passive joint,

## I. INTRODUCTION

Metamorphic mechanism is introduced in 1999[1]. Unlike traditional mechanism, metamorphic mechanism can change its configuration, mobility and the total number of all effective links during motions. The potential applications of this kind of mechanism are substantially large in terms of the application where the number of degree of freedom and geometric size are required to change, e.g., in space technology.

The spherical metamorphic mechanism is proposed as the revolving joint with spherical connection. Since the axis of the kinematics pair usually intersects at the same point, which allows the link to move on a spherical surface about the rotation center, and each link of these mechanism rotate about the point. Currently the study of spherical metamorphic mechanism involves the configuration analysis [2], mobility analysis [3], and structure synthesis [4]. The most problems of metamorphic mechanism joint have been avoided or ignored by researchers. This paper presents the Metamorphic Spherical Joint mechanism (MSJ), to avoid the problem of interference between mechanisms occupying the region of the center of rotation, it was decided to use a mechanism which would connect adjacent links, but which would have no part of the mechanism occupying the central region. That is, it should subtend the minimum possible angular area around the center of rotation. And the novel mechanism that allows multi links to be connected together and allows spherical motion about a rotation center. This mechanism is designed to be strong, rigid, easy to build, and have a large range of motion.

## II. PRIMARY DESIGN

The simplest spherical two-bar metamorphic mechanism is shown in Fig. 1, where one leaf is connected to a fixed support by a pin, the link is rigidly connected to the other leaf. The offset planar hinge gives one degree of freedom, while the pin through leaf “A” allows the offset hinge to pivot around its axis, providing a second degree of freedom. This allows the link B to move on a spherical surface about the center of rotation. If the link B is not connected rigidly to the leaf B, but is instead allowed to rotate about its long axis, the link B has three degrees of freedom. In this configuration, the link B moves as through it were connected to the center of rotation using a ball joint. The two links would then be able to move with respect to one another about the center of rotation with 3-DOF. Movement of the link B in the plane of the offset hinge is limited by the offset planar hinge limits discussed in section 4. The MSJ joint has three characteristic compare to traditional spherical joints. 1 The MSJ joint could connect multiple links compare to the traditional that connect two links. 2 It should subtend the minimum possible angular area around the center of rotation. 3 the MSJ joint is a passive joint.

### A. Planar Six-bar Linkage

Compare to the traditional rotary joint shown in Fig 2, A planar six-bar linkage is used to replace the rotary joint, which has the same center of rotation, but has no pivot at that point in Fig 3, that is, it should subtend the minimum possible angular area around the center of rotation, and obscure the minimum possible amount of the central region, this mechanism could be used to connect two links together, with addition rotary joints coaxial to each of the links.

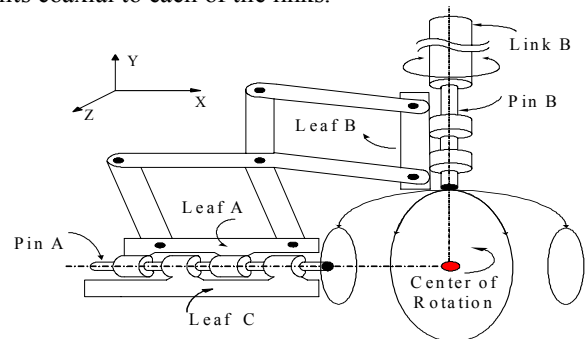


Fig. 1 A 3-DOF spherical joint

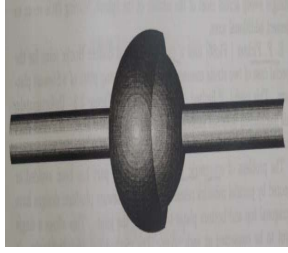


Fig. 2 Traditional rotary joint

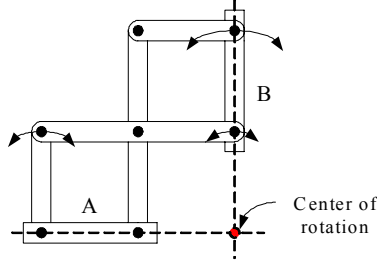


Fig. 3 Planar six-bar mechanism

### B. Offset Planar Hinge

The MSJ joint is assembled from one or more six bar linkages which will be referred to as offset planar hinges. An offset planar hinge is shown in Fig 4. The linkage is a type mechanism with two straight brackets, two bent brackets, and two leaves. Each leaf is one section of a hinge similar to a door hinge. This mechanism allows the two leaves to rotate with respect to one another about a fixed center of rotation in the plane. Compare to the planar six-bar mechanism in Fig. 3, this process is easiest to visualize if done in two steps. First, a bend is introduced into one of the members to shift the center of rotation of joint down by the desired offset distance. The linkage with this modification is shown in Fig 4. Note that the links still form parallelograms. At this point, one of the two link axes has been shifted by the offset amount. Next, a bend in the other long link introduce an offset for the other link axis. The final planar linkage, which will be called an offset planar hinges is shown in Fig.4. A line through the leaf, where the hinge pin would be placed, passes through the center of rotation. As shown in Fig. 1

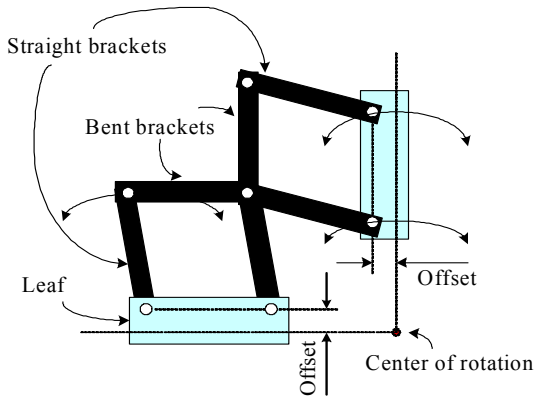


Fig. 4 The offset six-bar hinge model

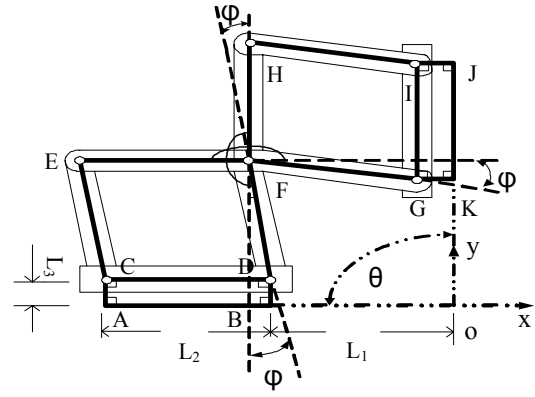


Fig. 5 Parameters of offset parallelograms

### C. Kinematics

As shown in Fig.5, three parameters  $L_1, L_2, L_3$  determine the dimension of the hinge. The bend in the long links are such that the point  $D$  and  $G$  are displaced from the lines  $HF$  and  $EF$  by the offset distance  $L_3$ . Points  $C, D, E, F, G, H$  and  $I$  are pivot points in the mechanism. Points  $A, B, J$  and  $K$  are the points on the axes of the two leaves. The bend in brackets  $DFH$  and  $EFG$  is specified by the angle  $\phi$ . Therefore, the closed loop mechanism form parallelograms, all of the dimension in the linkage are found to be the following:

$$\phi = \tan^{-1} \frac{L_3}{L_1} \quad (1)$$

$$|A-B| = |C-D| = |E-F| = |F-H| = |G-I| = |J-K| = L_2 \quad (2)$$

$$|C-E| = |D-F| = |F-G| = |H-I| = \sqrt{L_1^2 + L_3^2} \quad (3)$$

$$|A-C| = |B-D| = |G-K| = |I-J| = L_3 \quad (4)$$

The parallel links in the mechanism are shown follows:

$$\begin{aligned} \overline{AB} &\parallel \overline{CD} \parallel \overline{EF} \\ \overline{CE} &\parallel \overline{DF} \\ \overline{FH} &\parallel \overline{GI} \parallel \overline{JK} \\ \overline{FG} &\parallel \overline{HI} \\ \overline{AC} &\parallel \overline{BD} \\ \overline{GK} &\parallel \overline{IJ} \end{aligned} \quad (5)$$

The position of the mechanism may be parameterized by the angle  $\theta$ , which is the angle between  $\overline{AB}$  and  $\overline{JK}$ . To analyze the kinematics of the mechanism, the location of the point  $K$  is calculated as a function of  $\theta$ . It is shown that this point moves in a circle around the fixed center of a rotation as  $\theta$  is varied. A coordinate system is formed whose  $x$  axis lies along the line passing through the points  $A$  and  $B$ . The origin,  $O$ , of the coordinate system is located a distance  $L_1$  from the point  $B$  as shown in Fig. 5. From this point on, the symbols  $A, B$ , etc, will represent two dimensional vectors describing the position of the points in this coordinate system. Noting that the direction of the line from point  $G$  to point  $K$  is  $\frac{\pi}{2} - \theta$ , the location of point  $K$  is found as follows:

$$B = (-L_1, 0) \quad (6)$$

$$D = (-L_1, L_3) \quad (7)$$

$$F = D + \overline{DF}(\cos(\varphi + \pi - \theta), \sin(\varphi + \pi - \theta)) \quad (8)$$

$$\overline{DF} = \sqrt{L_1^2 + L_3^2} \quad (9)$$

$$G = F + (L_1, -L_3) \quad (10)$$

$$K = G + L_3(\cos(\frac{\pi}{2} - \theta), \sin(\frac{\pi}{2} - \theta)) \quad (11)$$

Put the equation (9) into (8), the location of  $F$  is determined, and the equation (8) into (10), the location of  $G$  is determined. Finally put the equation (10) into (11), the location of  $K$  is determined. The corresponding triangle are as follows (12), (13), (14), (15)

$$\sqrt{L_1^2 + L_3^2} = \frac{L_3}{\sin \varphi} \quad (12)$$

$$\tan \varphi = \frac{L_3}{L_1} \quad (13)$$

$$\cos(\pi + \varphi - \theta) = -\cos \varphi \cos \theta - \sin \varphi \sin \theta \quad (14)$$

$$\sin(\pi + \varphi - \theta) = -\sin \varphi \cos \theta + \cos \varphi \sin \theta \quad (15)$$

Put the equation (12), (13), (14), (15) into equation (11), and substitute the result in the following two expressions for the  $x$  and  $y$  components of  $K$ , after simplifying, the two equations become:

$$K_x = -L_1 \cos \theta \quad (16)$$

$$K_y = L_1 \sin \theta \quad (17)$$

### III. SPATIAL MECHANISM

For the same reason, If a second offset hinge were connected by one leaf to the movable link in the Fig. 1, and a second link connected to the free hanging leaf, And spherical 3-bar metamorphic mechanism is constructed in the Fig. 6, this mechanism be capable of deploying/folding, in the course of deploying/folding, both links would then be free to move on the same spherical surface about the same center of rotation. By connecting more offset hinges together, additional movable links can be added to the joint. Spherical 4-bar, spherical 5-bar, multi-bar metamorphic mechanism is constructed, due to the joint limits and joint workspace, the maximum link number is determined by the parameter  $L_1, L_2, L_3$ .

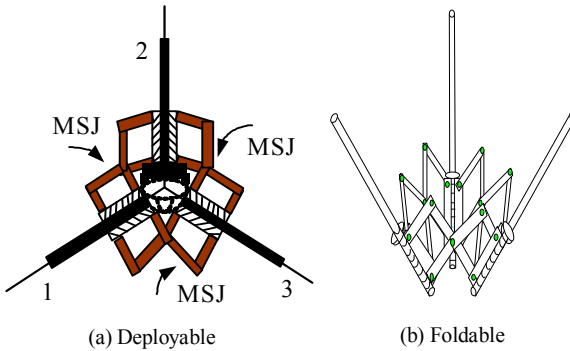


Fig. 6 Spherical 3-bars metamorphic mechanism

### IV. CONFIGURATION CHANGE

Metamorphic mechanism differs from traditional mechanism that has the facilities to change configuration from one kind to another, with a resultant change in the number of effective links and the mobility of movement during motions. The configuration changes of a spatial metamorphic mechanism can be formally described as a topological change with a set of matrix operation.

#### A. Joint limits

This MSJ joint is a kind of boundary-transformation metamorphic mechanism, each configuration change due to the joint limits:

- (1) the first limit is shown in Fig. 7. Rotation of the joint is stopped when the two hinge leaves contact at the point.
- (2) the second limit to the minimum offset planar hinge angle is shown in Fig. 8. this joint limit is caused when the two links connected to the same leaf collide.
- (3) the third limit to the dihedral angle joint limit in Fig. 9. These limits occur because of interference between multiple offset planar hinge leaves connected to the link which is shared by adjacent faces. Fig. 9 shows a view of a link along its axis, which indicates the point of contact between two adjacent offset planar hinges. This contact limits the minimum angle between two triangular faces in a spatial mechanism in the Fig. 6(b).

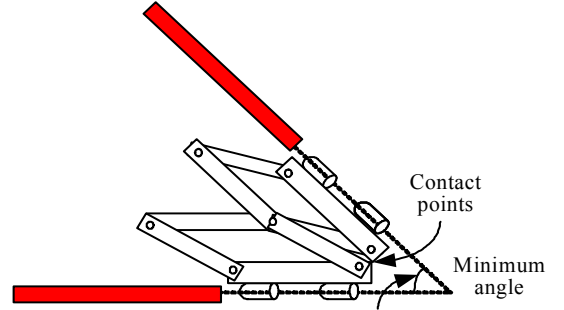


Fig. 7 The first limit

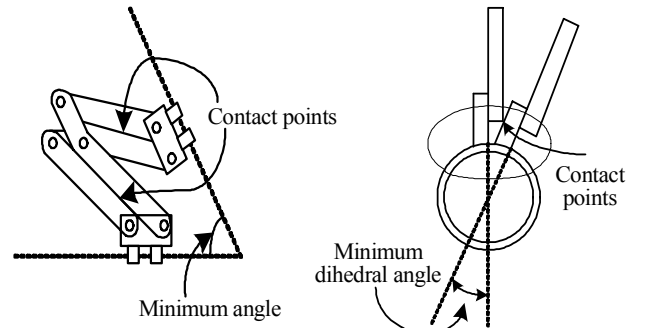


Fig. 8 The second limit

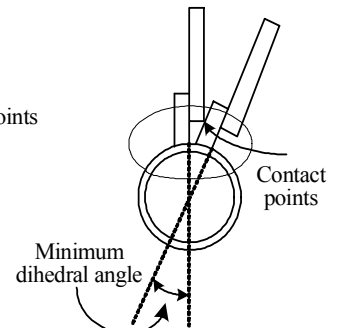


Fig. 9 The third limit

#### B. Degrees of Freedom

A degree of freedom analysis is one of the first steps necessary in studying a metamorphic mechanism. Fig. 10 shows a spherical six-bar metamorphic mechanism and its

topological graph, adjacent two links connected with MSJ, which composed of six MSJ joints and six links. On the assumption that the 1-link is fixed, the other links move on a spherical surface about the center of rotation, in this configuration, the link moves as though it were connected to the center of rotation using a ball joint. So each link have 3 DOF, and the DOF of spherical six-bar metamorphic mechanism is 15, due to the motion of the offset planar six-bar linkage, the 6<sup>th</sup> link moved close to the 1<sup>st</sup> link and stopped when the two hinge leaves contact at the point shown in Fig. 7, 8, the 6<sup>th</sup> link move to the limiting position, and the DOF of the 6<sup>th</sup> link cut down to 1, the residual DOF allows the 6<sup>th</sup> link to rotate about its long axis, then a spherical five-bar metamorphic mechanism come into being in Fig. 11, the DOF of this mechanism is 13. In the same manner, when the 5<sup>th</sup> close to the 6<sup>th</sup>, the 4<sup>th</sup> close to 5<sup>th</sup>, 3<sup>rd</sup> close to the 4<sup>th</sup>, a spherical four-bar, three-bar, two-bar metamorphic mechanism come into being in the Fig. 12, Fig. 13, Fig. 14, which shows the mechanism and its topological graph. the DOF of the four-bar, three-bar, two-bar, is 11, 9, 7. In the Fig. 14, the 1<sup>st</sup>, 3<sup>rd</sup>, 4<sup>th</sup>, 5<sup>th</sup> and 6<sup>th</sup> link consider to be one link, because each link relative to other link has no motion, and each link only have one DOF to spin about its axis without causing any motion of the mechanism. In the Fig. 14, the DOF of the 2<sup>nd</sup> link is 3, the first DOF results the 2<sup>nd</sup> link rotary joint coaxial with its axis, due to the two offset planar linkage which connect the 1<sup>st</sup> (3<sup>rd</sup>) and 2<sup>nd</sup>, the rest of DOF make the 2<sup>nd</sup> link move on a spherical surface about the center of rotation to the 1<sup>st</sup> (3<sup>rd</sup>, 4<sup>th</sup>, 5<sup>th</sup>, 6<sup>th</sup>) link. Finally, due to each MSJ moves to the limiting position shown in the Fig. 7, 8, 9. the spherical six-bar metamorphic mechanism composed of one link. Fig. 15 shows the detailed configuration change and the DOF'S change.

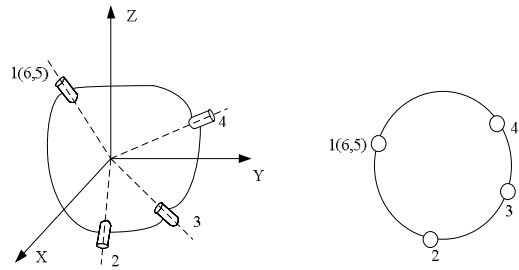


Fig. 12 Spherical four-bar

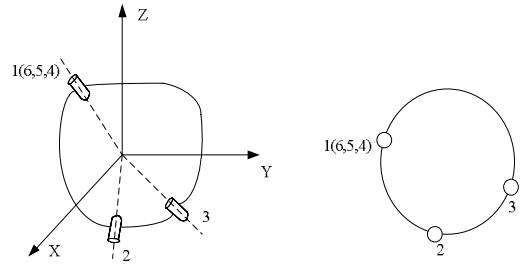


Fig. 13 Spherical three-bar

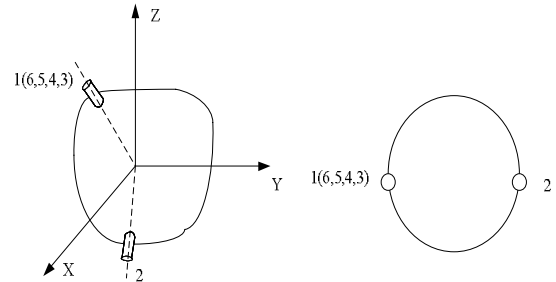


Fig. 14 Spherical two-bar

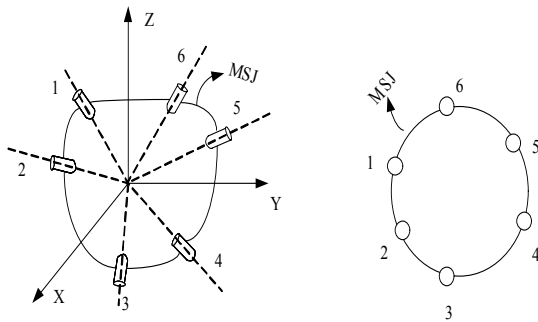


Fig. 10 Spherical six-bar

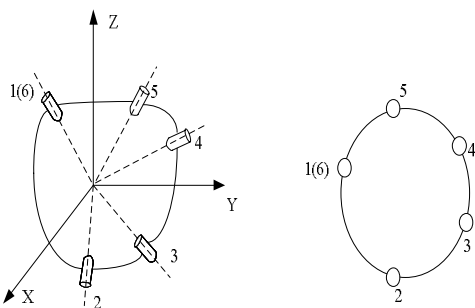


Fig. 11 Spherical five-bar

Configuration change	Topology graph	Steps for configuration change	DOF
Six-bar		Initial stage	15
Five-bar		The combination of link 6 and link 1	13
Four-bar		The combination of link 5, 6 and link 1	11
Three-bar		The combination of link 4, 5, 6 and link 1	9
Two-bar		The combination of link 3, 4, 5, 6 and link 1	7
Closed	One-bar without topology graph	The combination of link 2, 3, 4, 5, 6 and link 1	5

Fig. 15 Configuration change

### C. Configuration Analysis

To apply the graph theory, the node represent as link, the connection between two nodes represents as the kinematic pair. Spherical six-bar metamorphic mechanism and its topological graph are shown in the Fig. 10. The topological structure and link connectivity of a mechanism can be represented in a matrix form [5, 6, 7]. In the matrix, each link of the mechanism in its current configuration is identified by a number from 1 to  $n$ , the rows and columns of the matrix take these numbers in sequence. An entry of connectivity between the  $i$ th link and  $j$ th link is given as element  $(i, j)$  in an adjacency matrix. When two links are connected, the entry of corresponding row and column is given as 1. When two links are disconnected, the entry of the corresponding row and column is given as 0. This adjacency matrix of the six-bar configuration of the metamorphic mechanism in Fig. 10 is represented as  $A_0$ . The connectivity changes into a five-bar configuration as in Fig. 11 when links 6 and 1 of the six-bar configuration are attached together. For this changed topological configuration the adjacency matrix becomes  $A_1$ . As expected, this result in the change of both matrix elements and matrix order.

$$A_0 = \begin{matrix} & \begin{matrix} 1 & 2 & 3 & 4 & 5 & 6 \end{matrix} \\ \begin{matrix} 1 \\ 2 \\ 3 \\ 4 \\ 5 \\ 6 \end{matrix} & \begin{bmatrix} 0 & 1 & 0 & 0 & 0 & 1 \\ 1 & 0 & 1 & 0 & 0 & 0 \\ 0 & 1 & 0 & 1 & 0 & 0 \\ 0 & 0 & 1 & 0 & 1 & 0 \\ 0 & 0 & 0 & 1 & 0 & 1 \\ 1 & 0 & 0 & 0 & 1 & 0 \end{bmatrix} \end{matrix} \quad (18)$$

$$A_1 = \begin{matrix} & \begin{matrix} 1 & 2 & 3 & 4 & 5 \end{matrix} \\ \begin{matrix} 1 \\ 2 \\ 3 \\ 4 \\ 5 \end{matrix} & \begin{bmatrix} 0 & 1 & 0 & 0 & 1 \\ 1 & 0 & 1 & 0 & 0 \\ 0 & 1 & 0 & 1 & 0 \\ 0 & 0 & 1 & 0 & 1 \\ 1 & 0 & 0 & 1 & 0 \end{bmatrix} \end{matrix} \quad (19)$$

A topological change of mechanism represented in these two matrices thus take place. This topological change can be derived from an analytical way using an EU-elementary matrix operation on the initial adjacency matrix,  $A_0$ , to generate a new adjacency matrix  $A_1$ .

The EU-elementary matrix operation consist of the steps of applying a  $U_{i,j}$ -elementary matrix [8] operation and an elimination  $E_j$ -elementary matrix operation used in pairs. The function of the elementary matrix  $U_{i,j}$  in equation (20) and (21), (22) is to add the  $j$ th row to the  $i$ th row of an adjacency matrix when premultiplying an adjacency matrix, and it is embedded in the subscript. Postmultiplying the transpose of the elementary matrix adds the  $j$ th column to the  $i$ th column of the adjacency matrix. The new elementary matrix  $E_j$  in equation (20), and (21), (22) is introduced to perform the function of eliminating the  $j$ th row of an adjacency matrix when it is premultiplied to the adjacency matrix and eliminating the  $j$ th column when its transpose is postmultiplied to the adjacency matrix. Hence, the connectivity is passed on

and the number of links reduces. The use of these two matrix results in the EU-elementary matrix operation that performs the required configuration transformation. The matrix operation uses modular-2 arithmetic, sometimes known as exclusive-or arithmetic [9].

To transfer the six-bar configuration to five-bar configuration [10], an elementary matrix operation can be given

$$A_1 = (E_6 U_{1,6}) A_0 (E_6 U_{1,6})^T \quad (20)$$

where

$$E_6 = [I_5 \quad 0] = \begin{bmatrix} 1 & 0 & 0 & 0 & 0 & 0 \\ 0 & 1 & 0 & 0 & 0 & 0 \\ 0 & 0 & 1 & 0 & 0 & 0 \\ 0 & 0 & 0 & 1 & 0 & 0 \\ 0 & 0 & 0 & 0 & 1 & 0 \end{bmatrix} \quad (21)$$

$$U_{1,6} = \begin{bmatrix} 1 & 0 & 0 & 0 & 0 & 1 \\ 0 & 1 & 0 & 0 & 0 & 0 \\ 0 & 0 & 1 & 0 & 0 & 0 \\ 0 & 0 & 0 & 1 & 0 & 0 \\ 0 & 0 & 0 & 0 & 1 & 0 \\ 0 & 0 & 0 & 0 & 0 & 1 \end{bmatrix} \quad (22)$$

The above matrix operation in equation (20) can be decomposed into two steps. The first step is to apply the U-elementary matrix operation passing the connectivity of link 6 to link 1, This is completed by the matrix operation as shown in equation (22). The second step is to apply the E-elementary matrix operation to removed link 6 which is annexed to link 1. This is completed by the matrix operation as shown in equation (23).

$$A'_1 = U_{1,6} A_0 U_{1,6}^T = \begin{bmatrix} 0 & 1 & 0 & 0 & 1 & 1 \\ 1 & 0 & 1 & 0 & 0 & 0 \\ 0 & 1 & 0 & 1 & 0 & 0 \\ 0 & 0 & 1 & 0 & 1 & 0 \\ 1 & 0 & 0 & 1 & 0 & 1 \\ 1 & 0 & 0 & 0 & 1 & 0 \end{bmatrix} \quad (23)$$

$$A_1 = E_6 A'_1 E_6^T = \begin{bmatrix} 0 & 1 & 0 & 0 & 1 \\ 1 & 0 & 1 & 0 & 0 \\ 0 & 1 & 0 & 1 & 0 \\ 0 & 0 & 1 & 0 & 1 \\ 1 & 0 & 0 & 1 & 0 \end{bmatrix} \quad (24)$$

Hence, the five-bar configuration is obtained as  $A_1$  from the above decomposed elementary matrix operations. The above illustrative EU-elementary matrix operation can be extended to a complex metamorphic mechanism. The next topological configuration appears when the link 5 move to link 6(1) until the physical limit is reached, this configuration transformation can be represented by an  $E_5 U_{1,5}$  matrix operation, by the same way, when the link 4 move to link 5(1, 6), the link 3 move to the link 4(1, 6, 5), the configuration

transformation can be represented by an  $E_4U_{1,4}$ ,  $E_3U_{1,3}$  matrix operation. So the spherical four-bar, three-bar, two-bar, metamorphic mechanism is represented by the adjacency matrix  $A_2, A_3, A_4$  as shown in equation (25), (26), (27).

$$A_2 = \begin{bmatrix} 0 & 1 & 0 & 1 \\ 1 & 0 & 1 & 0 \\ 0 & 1 & 0 & 1 \\ 1 & 0 & 1 & 0 \end{bmatrix}, A_3 = \begin{bmatrix} 0 & 1 & 1 \\ 1 & 0 & 1 \\ 1 & 1 & 0 \end{bmatrix}, A_4 = \begin{bmatrix} 0 & 1 \\ 1 & 0 \end{bmatrix} \quad (25)$$

## V. APPLICATION

Section 4 discusses how the offset planar hinge linkage is connected together to form spatial mechanism which act as spherical joints. Compare with traditional spherical joint, these spatial linkage allow multiple links to be connected together with a common center of rotation. To apply the MSJ joint to the variable geometry truss manipulator, the simplest 3D truss is the tetrahedron, with six links connected to four nodes. At each node three links are met at a point. If the truss is actuated, then the links must be connected together in a manner that allows spherical motion of the links about the vertices of the tetrahedron. Connecting three offset hinges together as shown in Fig. 6, forms the three link MSJ joint required for such a tetrahedral robot. The leaves of adjacent offset hinge are attached together by passing pins through them, in the manner of a door hinge. The links are connected to these pins. Four of these joints may be connected together with six links to form a tetrahedron in the Fig. 16, use 7 tetrahedron to form a 7-celled tetrahedral variable geometry truss robotics manipulator in the Fig. 17, which is composed of 7 tetrahedral modules, 10 nodes, and 7 actuated links, the 10 nodes can be classified into 3 fixed base nodes ( $n_1, n_2, n_3$ ), 3 controlled nodes ( $n_8, n_9, n_{10}$ ), and 4 unconstrained nodes ( $n_4, n_5, n_6, n_7$ ), the fixed module is connected to a support by the three “fixed” nodes, and the “last” module in the chain act as the end-effector. The actuated links is  $l_{41}, l_{52}, l_{63}, l_{74}, l_{85}, l_{96}, l_{10,7}$ , which are lead-screw type electric linear actuator. the planar 8–9–10 is work platforms, in this truss mechanism, all of the links are two force members which only experience tension or compression type forces along the axis of the link. The spherical metamorphic mechanism joint may be used to construct a wide variety of robot mechanisms. These mechanisms could be arms, manipulator, vehicles, supports, or could characteristics of these and other robots. Just as the configuration can change, so can the applications.

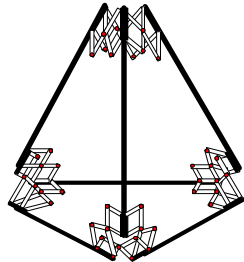


Fig. 16 A tetrahedral truss with three axis joints

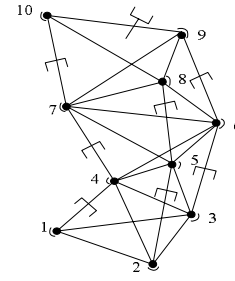


Fig. 17 Configuration of 7 tetrahedral modules

## VI. CONCLUSION

This paper proposes a metamorphic spherical joint. With this MSJ joint, a spherical 6-bar metamorphic mechanism is introduced, DOF analysis and the configuration change have also been explained. It is an innovative mechanism design to introduce this MSJ to variable geometry truss manipulator. Comparing to the conventional spherical joint, MSJ has three advantages. (1) MSJ can connect multiple links comparing to the conventional scheme that can connect two links only. (2) When this joint is used to a variable geometry truss manipulator, the MSJ avoid the joint limits and joint interference. (3) MSJ can be used to design module mechanism to construct multiple polyhedron variable geometry truss manipulator.

## ACKNOWLEDGMENT

This work is supported by Natural Science Foundation of China under the research project 60775059, 50375008, and 863 Program of China under the research project 2006AA04Z218

## REFERENCES

- [1] J. S. Dai, Rees Jones John, “Mobility in Metamorphic Mechanisms of Foldable/Erectable Kinds,” Transaction of ASME, Journal of Mechanical Design, Vol. 121, Issue 3, May 1999, pp.375-382
- [2] N. V. Dubey, J. S. Dai, K. Stamp, and J. R. Jones, “Kinematic Simulation of a Metamorphic Mechanism,” Proc. of Tenth World Congress on the Theory of Machines and Mechanism,” Oulu, Finland, 1999, pp. 98-103
- [3] J. S. Dai, Q. X. Zhang, “Metamorphic Mechanisms and Their Configuration Models,” Chinese Journal of Mechanical Engineering, Vol. 13, No. 3, 2000, pp.212-218
- [4] D. L. Li, “Analysis and Application of Metamorphic Mechanism,” PhD Thesis, Beijing University of Aeronautics & Astronautics, China, 2003.
- [5] J. S. Dai, and J. R. Jones, “Matrix Representation of Topological Changes in Metamorphic Mechanisms,” Journal of Mechanical Design, Vol. 127, Issue 4, July 2005, pp. 837-840
- [6] J. M. Rico Martinez, and B. Ravani, “On Mobility Analysis of Link ages Using Group Theory,” ASME J. Mech. Des., 125, 2003, pp.70-80.
- [7] Q. Jin, and T. L. Yang, “Synthesis and Analysis of a Group of 3-Degree-of-Freedom Partially Decoupled Parallel Manipulator,” Journal of Mechanical Design, Vol. 126, Issue 2, Mar. 2004, pp.301-306
- [8] G. Strang, “Linear Algebra and Its Application,” 2<sup>nd</sup> Ed, Academic, New York, 1980.
- [9] A. C. Gillie, “Binary Arithmetic and Boolean Algebra,” McGraw-Hill, New York, 1965,
- [10] S. S. Balli, and S. Chand, “Synthesis of a Five-Bar Mechanism of Variable Topology Type With Transmission Angle Control,” Journal of Mechanical Design, Vol. 126, Issue 1, Jan. 2004, pp.128-134
- [11] T. L. Yang, “Basic Theory of Machine System-Structure, Kinematics, Dynamics,” Machine Industry Press, Beijing, China, 1996
- [12] Q. X. Zhang, “Analysis and Synthesis of Space Mechanism,” Machine Industry Press, Beijing, China, 1984